Scholar Publishing Group
International Journal of Neural Network
https://doi.org/10.38007/NN.2021.020404
ISSN 2790-2692 Vol. 2, Issue 4: 24-31

Roughness Prediction Model Based on Neural Network

Hong Yang*

Qinghai Normal University, Qinghai, China

1756359616@qq.com

**corresponding author*

Keywords: Neural Network, Surface Roughness, Predictive Model, Model Analysis

Abstract: In order to meet the needs of people's consumption quality upgrade, major manufacturers have put forward higher requirements for the machining accuracy, surface roughness and material properties of the workpiece. By building a prediction model (PM) to predict the surface of the formed parts with different process parameters Roughness, using NN to build a roughness prediction model (PM), adjust the process parameters through the model, and ensure the surface quality of the parts. Therefore, this paper discusses and studies the roughness PM based on neural network (NN). This paper firstly introduces the basic situation of the surface topography simulation system and the workflow of the PM in detail, and then builds the PM from the surface roughness measurement, data processing and overall parameter design, and finally compares the model results. Analysis and evaluation index analysis.

1. Introduction

With the development of economy, people's living standards have been greatly improved, people pay more and more attention to the quality of consumer goods, and the consumption structure is changing [1]. The early roughness PM mainly uses mathematical modeling to build the model, but this method can only simply reflect the linear relationship between the target quantity and the influencing factors, and it is easy to ignore the comprehensive influence of each factor [2-3]. Later, representative experimental data were used to build a surface roughness PM, but the prediction accuracy of the model was low [4]. Optimizing and improving the NN PM can improve the accuracy of the nonlinear relationship between the target quantity and the input quantity, and promote the development of material technology [5].

At present, there are many roughness PMs based on NN, and the prediction accuracy and efficiency are also different [6]. For example, researchers such as Villegas J have proposed a deep convolutional NN-based method to classify surface roughness in response to the problem that machine vision roughness detection is highly dependent on the light source environment. With good light source robustness, roughness detection can be achieved without design metrics, and the research adopts an end-to-end image analysis method to finally achieve the classification and

prediction of surface roughness [7]. Experts such as Mulay A used the NN to establish the relationship between grinding parameters and surface roughness, and used the globally optimized processing parameters for the experiment, and finally obtained the surface roughness of the cycloid gear. By comparing the two experimental results, the two surface roughnesses the degree of error is 2.06%, and the NN can effectively predict the surface roughness of the cycloid gear after grinding [8]. However, in recent years, the research results of roughness PM based on NN are few, and researchers should pay attention to the development and research of NN PM.

Whether the surface roughness PM can be accurately predicted is related to the development of material technology in the manufacturing industry, so this paper discusses the roughness PM based on NN. The content of the research part of this paper can be divided into three parts: the first part is the relevant overview part, mainly including the surface topography simulation system and the PM workflow; the second part is the construction of the PM, which is based on the NN construction of the The NN PM builds the PM according to the three aspects of surface roughness measurement, data processing and overall parameter design; the third part analyzes the PM, and analyzes the model from the perspectives of model results and evaluation indicators. Draw relevant conclusions.

2. Related Overview

2.1. Surface Topography Simulation System

The main function of the simulation system is to establish a mathematical model of the actual machining problem, set constraints according to the machining conditions, determine the optimization target according to the workpiece performance index, and use the genetic algorithm to obtain the optimal milling parameter combination [9]. The system includes modules such as practical problem modeling, constraint setting, optimization objective selection, genetic algorithm calling, and optimization result display. It can perform single-objective or multi-objective optimization, and select different optimization objectives or different constraints for parameter optimization. Moreover, the optimization results can be used for surface topography simulation [10-11]. The structure of the simulation system is shown in Figure 1.

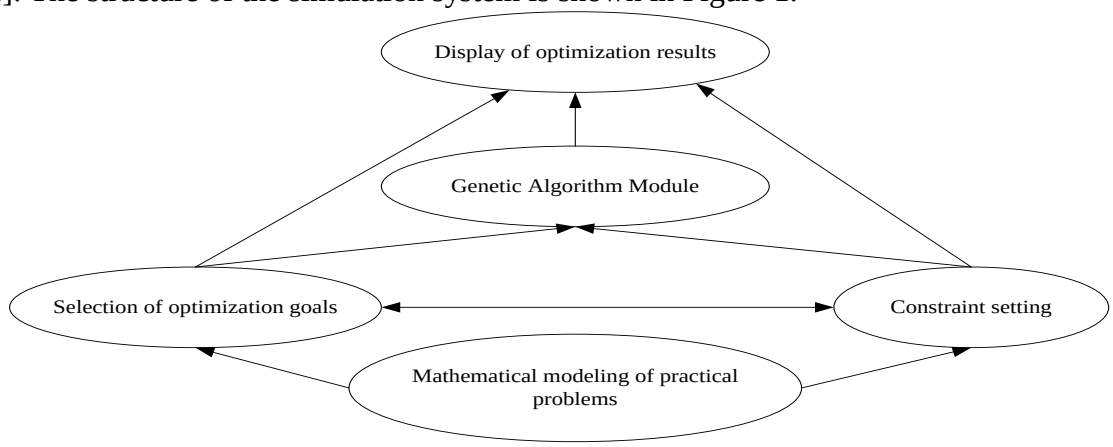

Figure 1. Simulation system structure diagram

The functions of each module of the system are described as follows:

Actual problem modeling: The actual processing problem is digitally modeled, and the ultimate goal of parameter optimization is to maximize the benefits under the premise of ensuring the quality of parts processing, and set the parameters as variables for modeling [12].

Select the optimization target: According to the demand, the optimization target can be set as

single or multiple. That is, the maximum productivity Q or the minimum surface roughness Ra can be set as a single optimization objective function respectively, or can also be set as multiple optimization objective functions for comprehensive optimization.

Setting constraints: The actual processing conditions can be input in the relevant modules of the system interface [13].

Genetic Algorithm Module: Genetic Algorithm module is the core structure of the system. It can write specific fitness function M files to expand and improve Matlab's built-in genetic algorithm toolbox GAOT [14].

Display of optimization results and surface topography: Through the operation, the interface will display the optimized parameters, which are compared with the original parameters. In the interface operation bar, the surface topography simulation function is set, and the optimal parameters can be used as input to obtain the surface topography of the part, and the related information such as the surface processing quality of the part can be more intuitively displayed [15-16].

2.2. Predictive Model Workflow

In this paper, through the experimental data under different process conditions, a NN model with different process parameters as input and surface roughness as output is gradually established, and the surface roughness of the corresponding workpiece can be predicted according to the given combination of process parameters. The model building process is shown in Figure 2.

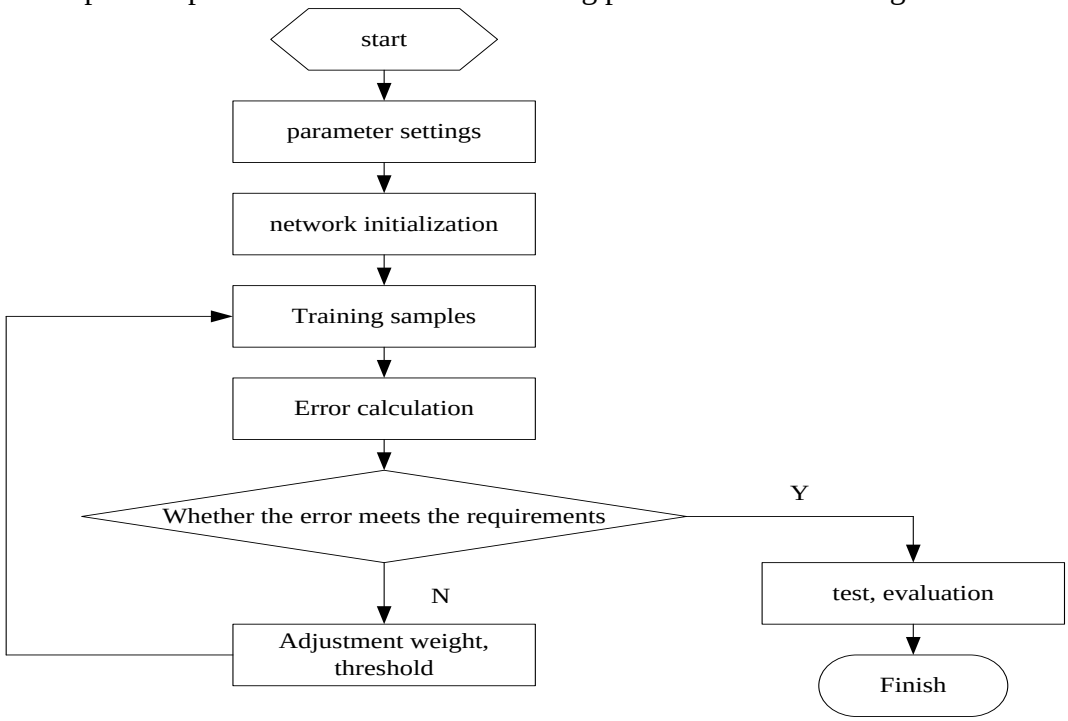

Figure 2. Model workflow flowchart

3. Model Building

3.1. Measurement of Surface Roughness

The state of the workpiece after machining can be described by two concepts: one is the concept of machining quality, and the other is the concept of surface integrity [17]. Since the surface roughness index appears in the above two concepts, it can be seen that it plays an important role in

evaluating the quality of the processed parts. The concept of surface roughness is mainly used for the microscopic state of the surface of the parts after processing, that is, the degree of surface unevenness. The more obvious the concave-convex state of the workpiece surface is, the larger the value is, the rougher the workpiece surface is, and vice versa [18]. The evaluation parameters of surface roughness are mostly Ra and Ry. In this paper, Ra value is selected as the index of surface roughness value.

Use a surface roughness measuring instrument to obtain the measured value Ra of the surface roughness of the workpiece. Since the Ra value is greatly affected by the material properties, it is not only related to the structure, but also to the orientation. The surface roughness Ra values measured in different measurement directions are shown in Table 1.

Table 1. Surface roughness measurement value Ra (μm) in different measurement directions

	1	2	3	4	5	6	7	8	9
45 °	2.469	2.743	2.949	2.543	2.687	2.654	2.113	2.242	2.416
90 °	3.145	3.876	4.375	3.753	3.291	2.989	2.164	2.976	3.154
135 °	2.176	2.451	2.634	2.312	2.143	1.845	2.087	2.145	2.243

It can be seen from Table 1 that the variation trend of the surface roughness measurement value Ra is the same in different measurement directions, but under the same processing conditions, the measurement value Ra fluctuates between 1.845 μm and 4.375 μm; when the measurement direction is 90°, the maximum measurement value Ra is the largest. The value of Ra is 4.375μm, the minimum value is 2.164μm, the fluctuation range of Ra reaches 2.211μm, and the fluctuation range of Ra is controlled within 1μm when the measurement direction is 45 ° and 135 °, indicating that the measurement direction has a greater impact on the Ra value.

3.2. Data Processing

In order to obtain the features of real sample figures and generated sample figures, we build a deep autoencoder network to automatically extract data features. First, the deep autoencoder network is pre-trained with the real surface roughness sample data ri, and the network parameters for extracting figure features are obtained. After the pre-training is completed, the features Fi of the real data can be obtained. We share the trained network parameters into the convolutional NN, so that the convolutional NN has the ability to extract data features. Then, input the uniformly distributed noise vector Z into the generator network of GAN, and output the generated sample data ki; input ki into the convolutional NN to obtain the feature Gi of the generated data. There are two HLs in the deep autoencoder in this paper, and the specific process is as follows:

$$F_i = f_{\theta_2}\left(W_2 f_{\theta_2}\left(W_1 r_i + b_1\right) + b_2\right) \tag{1}$$

$$G_i = f_{\theta_2}\left(W_2 f_{\theta_1}\left(W_1 k_i + b_1\right) + b_2\right) \tag{2}$$

Where θ1 and θ2 are the parameter group of DAE from the input layer to the group (HL) and from the HL to the output layer respectively, W1 and W2 are the weight matrices, and b1 and b2 are the bias vectors.

3.3. Overall Parameter Design

The working performance of the PM is studied. The value of the number of HL nodes m is 4, 5, 6, 7, 8, 9 and 10. The selected reference quantities are the number of iterations, the prediction accuracy, and the fit value. The results are shown in the table. 2 shown.

Table 2. Model prediction results for different HL nodes

Number of hidden nodes	Iterative convergence times	Prediction accuracy	Fit	
			Maximum value	minimum
4	57	1.78×10^{-3}	0.926	0.732
5	58	6.54×10^{-4}	0.895	0.686
6	52	2.21×10^{-3}	0.972	0.961
7	51	5.63×10^{-4}	0.896	0.654
8	51	4.52×10^{-3}	0.865	0.746
9	56	4.61×10^{-3}	0.902	0.812
10	59	4.32×10^{-3}	0.859	0.713

By analyzing the prediction results in Table 2, we can get:

When the same PM selects HL with the same number of layers but different nodes, the iterative convergence steps of the PM are different. When the number of nodes (TNON) is 4 and 5, the number of convergence steps is more. When TNON is 7 and 8, the fastest convergence speed can reach 51 steps. When TNON is 6, the model iterates 52 times and completes the convergence. When it is 10, the number of iteration steps increases and the convergence speed decreases.

Observe the effect of different HL nodes on the prediction accuracy and fit of the same sample. When TNON is 5 and 7, the prediction accuracy is the lowest. When TNON is 7, the maximum fitting level is 0.896 and the minimum fitting level is 0.654, indicating that the tracking ability of different samples is different and the difference is relatively high. big. When TNON is 6, its prediction accuracy value is higher than that of other nodes, and the difference between the maximum and minimum fit is the smallest. Therefore, the number of HL nodes in this paper is 6.

4. Model Analysis

4.1. Comparative Analysis of Model Results

In this paper, LSTM-CNN PM, BIGRU-CNN PM and BILSTM-CNN PM are respectively constructed based on NN. After the training of the three PMs is completed, 11 sets of verification samples are input, and they are respectively investigated from the perspective of prediction accuracy. Working performance, Figure 3 is a comparison chart of the error between the predicted date and the measured date of the three PMs.

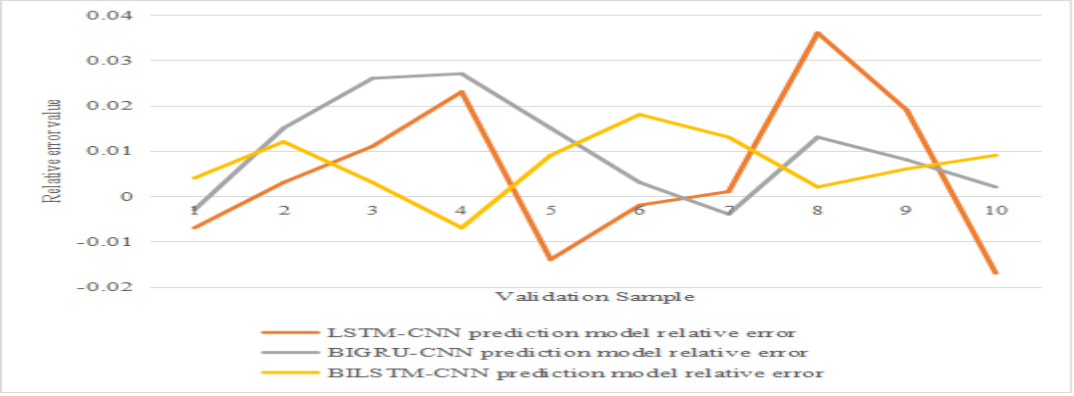

Figure 3. Comparison of the error between the models predicted value and the measured value

As can be seen from Figure 3, the error range of the LSTM-CNN PM image Y value is -0.017μm to 0.036μm, the BIGRU-CNN PM image Y value error range is -0.003μm~0.027μm, BILSTM-CNN predicts The error range of the Y value of the model image is between -0.007 μm and 0.018 μm. By comparing the errors of the three models, it can be seen that the prediction range of the BILSTM-CNN PM is the smallest, indicating that the prediction value of the BILSTM-CNN PM is closer to the measured data, and the prediction accuracy of the model is strong.

4.2. Analysis of Evaluation Indicators

The PMs were compared and analyzed using the evaluation indicators RMSE and MAE. Two stacked 1DCNN layers are added before LSTM, GRU, bidirectional LSTM and bidirectional GRU. The statistical evaluation index RMSE value and MAE value of the experimental results are shown in Figure 4. It can be seen from Figure 4 that the RMSE and MAE values of the LSTM-CNN model are 8.11 and 5.83, respectively; the RMSE value of the GRU-CNN PM is 8.98 and the MAE value is 6.75; the RMSE and MAE values of the BILSTM-CNN model are 6.64 and 4.47, respectively. ; The BIGRU-CNN PM has an RMSE value of 7.57 and an MAE of 5.12. Comparing and analyzing the four models, it is found that the RMSE and MAE values of the LSTM-CNN are the smallest, indicating that the model has the best prediction effect, followed by the BIGRU-CNN model. Using CNN to extract local spatial features can not only effectively filter out the noise of the original sequence, but also shorten the length of the original sequence and make it a short sequence composed of local features, which can make the following bidirectional LSTM and bidirectional GRU better capture timing characteristics.

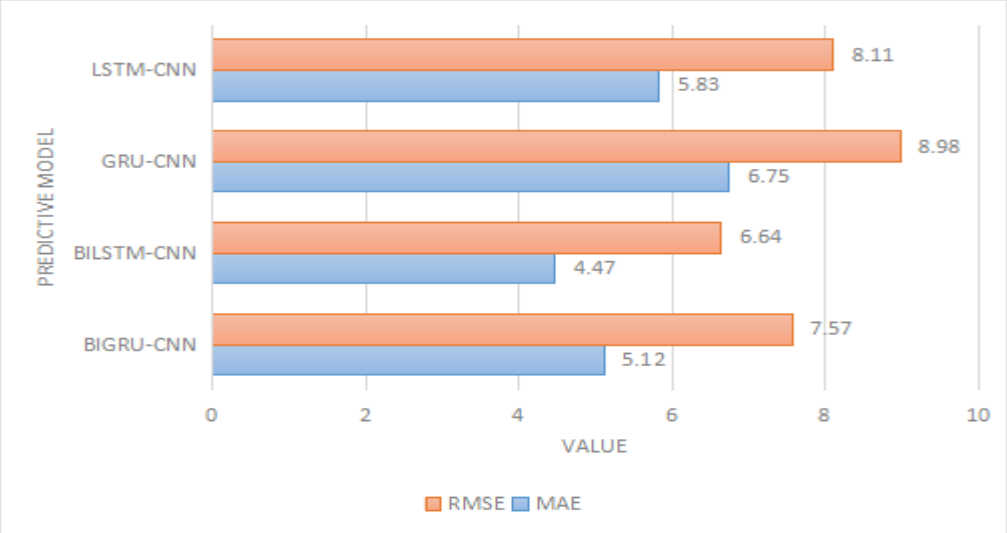

Figure 4. Comparison of evaluation index models

5. Conclusion

In view of the fact that the traditional CNC grinding needs to adjust the processing parameters many times to meet the surface roughness value specified in the drawing, and the process of adjusting the parameters must be accompanied by a decrease in productivity and a decrease in the accuracy of the workpiece, in order to meet the requirements of high precision and high productivity at the same time. The research on the PM of the workpiece surface roughness after processing based on the given processing parameters has been widely concerned. This paper builds a PM based on NN, and draws the following conclusions through the analysis of the model. Through model comparison and analysis, it is found that the predicted value of the BILSTM-CNN

PM is closer to the measured data, and the prediction accuracy is strong; using the RMSE and MAE evaluation indicators analysis, it is found that the RMSE and MAE values of the LSTM-CNN model are both the smallest. most. Due to the limited professional ability of this paper, there are many deficiencies in the research process that need to be improved.

Funding

This article is not supported by any foundation.

Data Availability

Data sharing is not applicable to this article as no new data were created or analysed in this study.

Conflict of Interest

The author states that this article has no conflict of interest.

References

[1] Fakhri M, Dezfoulian R S. Pavement structural evaluation based on roughness and surface distress survey using NN model. Construction and Building Materials, 2019, 204(2019):768-780. https://doi.org/10.1016/j.conbuildmat.2019.01.142

[2] Daoud O A, Ksaibati K. Artificial NN-based roughness prediction models for gravel roads considering land use. Innovative Infrastructure Solutions, 2022, 7(3):1-11. https://doi.org/10.1007/s41062-022-00793-0

[3] Abdulateef O F. Surface Roughness Prediction in Turning Operation of Aluminum Alloy 6061using Artificial NN (Ann). Journal of Mechanical Engineering Research and Developments, 2020, 43(4):360-366.

[4] Jankovic P, Madic M, Radovanovic M, et al. Optimization of Surface Roughness from Different Aspects in High-Power CO_2 Laser Cutting of AA5754 Aluminum Alloy. Arabian Journal for Science and Engineering, 2019, 44(12):10245-10256. https://doi.org/10.1007/s13369-019-04037-9

[5] Maleki M, Amini J, Notarnicola C. Soil Roughness Retrieval from TerraSar-X Data Using NN and Fractal Method. Advances in Space Research, 2019, 64(5):1117-1129. https://doi.org/10.1016/j.asr.2019.04.019

[6] Khadar S. Evaluation of surface roughness in the turning of mild steel under different cutting conditions using backpropagation NN. Proceedings of the Estonian Academy of Sciences, 2020, 69(2):109-115. https://doi.org/10.3176/proc.2020.2.02

[7] Villegas J, Markov K, Perkins J, et al. Prediction of Creaky Speech by Recurrent NNs Using Psychoacoustic Roughness. IEEE Journal of Selected Topics in Signal Processing, 2020, 14(2):355-366. https://doi.org/10.1109/JSTSP.2019.2949422

[8] Mulay A, Ben B S, Ismail S , et al. Prediction of average surface roughness and formability in single point incremental forming using artificial NN. Archives of Civil and Mechanical Engineering, 2019, 19(4):1135-1149. https://doi.org/10.1016/j.acme.2019.06.004

[9] Pourseiedrezaei M, Loghmani A, Keshmlri M. Prediction of Psychoacoustic Metrics Using Combination of Wavelet Packet Transform and an Optimized Artificial NN. Archives of acoustics, 2019, 44(3):561-573.

[10] Erygin E, Duyun T. Development of Nns for Forecasting Roughness When Milling Various

Materials. Bulletin of Belgorod State Technological University named after V G Shukhov, 2020, 5(11):113-124. https://doi.org/10.34031/2071-7318-2020-5-11-113-124

[11] Beemaraj R K, Sekar M, Vijayan V. Computer vision measurement and optimization of surface roughness using soft computing approaches:. Transactions of the Institute of Measurement and Control, 2020, 42(13):2475-2481. https://doi.org/10.1177/0142331220916056

[12] H Gürbüz. Estimation of surface roughness and cutting speed in CNC WEDM by artificial NN that employed trainable activation function. Proceedings of the Institution of Mechanical Engineers, Part C: Journal of Mechanical Engineering Science, 2021, 235(15):2737-2753. https://doi.org/10.1177/0954406221990057

[13] Vagheesan S, Govindarajalu J. Hybrid NN–particle swarm optimization algorithm and NN–genetic algorithm for the optimization of quality characteristics during CO 2 laser cutting of aluminium alloy. Journal of the Brazilian Society of Mechanical Sciences and Engineering, 2019, 41(8):1-15. https://doi.org/10.1007/s40430-019-1830-8

[14] Naguib A, El-Badawy S, Ibrahim M. International Roughness Index Predictive Model for Rigid Pavements based on LTPP Data(Dept. C (PUPLIC)). Bulletin of the Faculty of Engineering Mansoura University, 2020, 40(2):30-38. https://doi.org/10.21608/bfemu.2020.101239

[15] Getmanov V G , Chinkin V E , Sidorov R V , et al. Geomagnetic Storm Prediction Based on the NN Digital Processing of Joint Observations of the URAGAN Muon Hodoscope and Neutron Monitor Stations. Geomagnetism and Aeronomy, 2022, 62(4):388-398. https://doi.org/10.1134/S0016793222040089

[16] Galati M, Rizza G, Defanti S, et al. Surface roughness prediction model for Electron Beam Melting (EBM) processing Ti6Al4V. Precision Engineering, 2021, 69(2):19-28. https://doi.org/10.1016/j.precisioneng.2021.01.002

[17] Kayser B, Gauvreau B, D Ecotière. Sensitivity analysis of a parabolic equation model to ground impedance and surface roughness for wind turbine noise. The Journal of the Acoustical Society of America, 2019, 146(5):3222-3231. https://doi.org/10.1121/1.5131652

[18] Ramesh P, Mani K. Prediction of surface roughness using machine learning approach for abrasive waterjet milling of alumina ceramic. The International Journal of Advanced Manufacturing Technology, 2022, 119(1):503-516. https://doi.org/10.1007/s00170-021-08052-9